E-ISSN 2586-9027
Homepage : https://tci-thaijo.org/index.php/SciTechAsia Science & Technology Asia
Vol.30 No.4 October - December 2025 Page: [230-242]
*Original research article*

# Computational Fluid Dynamics Simulation Of T-Pipe Scaling Up With Heavy Oil-Water Core-Annular Flow

Muhammad Erzaditya Zhafran, Cindy Dianita*

*Department of Chemical Engineering, Faculty of Engineering, Universitas Indonesia, Depok 16424, Indonesia*

Received 5 June 2025; Received in revised form 28 August 2025
Accepted 17 September 2025; Available online 17 December 2025

**ABSTRACT**

Core annular flow (CAF) offers significant energy savings for transporting heavy oils, but its large-scale application in complex geometries remains poorly understood. This study investigates the scale-up of CAF in a T-shaped pipe (T50-50) with water insertion using computational fluid dynamics (CFD). The objective is to evaluate the effects of Reynolds number (Re), Bingham number (Bi), and Froude number (Fr) on flow stability, fouling, and energy efficiency. Simulations employed the Volume of Fluid (VOF) method with the Carreau model to capture shear-thinning behavior. Pipe dimensions were scaled by factors of 1.5 and 5, and performance was assessed through pressure gradient, oil holdup, and energy savings. Results show that maintaining Fr > 1 is essential for concentric CAF stability and fouling reduction. At 1.5× scale-up, oil holdup errors relative to theory were 0–19%, while pressure gradient errors were 19–52%. At 5×, errors increased sharply, particularly under Reynolds scaling (up to 554%). Despite this, CAF consistently reduced pumping energy by more than 80%, reaching 98–100% savings. In conclusion, CAF remains an effective strategy for heavy oil transport, with Fr governing stability and Bi providing the best predictor of energy efficiency.

**Keywords:** Core Annular Flow (CAF); Computational Fluid Dynamics (CFD); Dimensionless parameter; Scale up; T-pipe

## 1. Introduction

The transportation of heavy and viscous oil presents significant challenges, including high pumping power requirements, severe pressure drops, and environmental concerns. Compared to non-viscous oil, the

***Corresponding author:** cindydianita@ui.ac.id **doi:** 10.14456/scitechasia.2025.81

distribution of viscous oil demands substantially higher costs and energy consumption. To address these inefficiencies, Core Annular Flow (CAF) technology has emerged as a promising method, where a high-viscosity fluid is transported as the core surrounded by a lubricating low-viscosity fluid. This configuration drastically reduces friction and power consumption, offering potential energy savings of over 80% relative to single-phase transport methods [2].

Extensive research has been conducted to understand and optimize CAF. Prior studies have examined its formation and stability in small-scale geometries using both experiments and computational fluid dynamics (CFD) simulations [4–6]. For example, Dianita et al. [5] investigated CAF in T- and Y-shaped pipes with diameters of 20 mm and 50 mm, showing that flow stability is strongly influenced by geometry. While the T50-50 configuration maintained CAF more effectively than other geometries, fouling zones were observed near branching regions. To mitigate this, further studies introduced additional water insertion at pipe branches, which partially restored the CAF pattern [6]. Despite these advances, most investigations have been limited to laboratory-scale systems, and their direct application to industrial-scale pipelines remains uncertain. In particular, the scale-up of CAF in branching pipe configurations—common in real-world oil transportation networks—has not been systematically addressed.

The scaling of CAF is further complicated by the non-Newtonian nature of heavy oil, which often exhibits shear-thinning behavior. Such rheological effects increase the likelihood of instability, fouling, and pressure losses in large-scale systems [11]. While previous work has considered scaling in horizontal pipes with sudden expansion [7] and explored parameter variations such as Reynolds number [8], there remains a lack of comprehensive studies combining multiple dimensionless parameters to guide scale-up in branched geometries. This gap limits the ability to predict stable CAF performance in industrial applications.

To bridge this gap, the present study investigates the scale-up of the T50-50 pipe configuration with additional water insertion, building directly on the geometry established by Dianita et al. [6]. Using CFD simulations, this research systematically evaluates the influence of key dimensionless parameters—Reynolds number (Re), Bingham number (Bn), and Froude number (Fr)—on CAF formation, stability, and fouling behavior. Importantly, the study employs the Carreau model to capture the shear-thinning rheology of heavy oil, ensuring more accurate representation of non-Newtonian effects compared to prior scale-up studies that relied on simplified assumptions.

The novelty of this study lies in scaling up core annular flow (CAF) in T-junction pipes beyond laboratory dimensions, specifically addressing junction-induced instabilities that are most severe at larger scales. In addition, the study integrates non-Newtonian rheology through the Carreau model to more realistically capture the shear-thinning behavior of heavy oil. Furthermore, it quantitatively evaluates key dimensionless parameters—Reynolds number (Re), Bingham number (Bi), and Froude number (Fr)-as scale-up criteria, thereby providing new insights into flow stability and fouling tendencies that have not been systematically analyzed in prior works. Through this approach, the research delivers practical design guidelines for scaling CAF systems from experimental setups to industrial applications, ultimately

enhancing the feasibility of energy-efficient heavy oil transportation.

## 2. Materials and Methods

### 2.1 System description

Simulation data for CAF is based on Dianita et al. [6] and fluid properties are referenced from Montes et al. [14]. The required simulation data includes:

1. Fluid Properties (Viscosity and Density)
2. Pipe Geometry (Diameter, Length, and Type of Pipe)
3. Fluid Conditions (Flow Rate)

are carried out with pre-processing, which involves creating geometry of T pipe with similar inlet and outlet diameter i.e., 50 mm (coded as T50-50) modified with ducting insertion (coded as DI 2-8) [6] illustrated by Fig. 1.

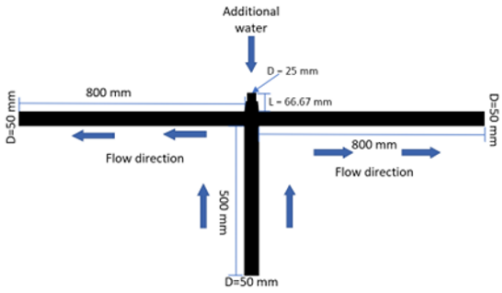


**Fig. 1.** Geometry T50-50 DI-2-8.

After completing the geometry, meshing is performed in ANSYS with an adjustable number of mesh cells. Once the geometry and mesh are finalized, the simulation advances to the solving phase, where fluid data and simulation parameters are defined. The system then executes the simulation using various methods available during the solution phase. Convergence is essential before moving to the result processing stage. If convergences are not achieved, the mesh count has to be adjusted and the simulation must be repeated. Upon achieving convergence, the results are validated against experimental models during post-processing. Discrepancies are addressed by refining the simulation parameters and running it again. Satisfactory results lead to the scaling-up phase, where pipe dimensions are increased to 1.5× and 5× the original size.

### 2.2 System parameter

The numerical simulation of multiphase flow dynamics was carried out using the Volume of Fluid (VOF) approach, where water was designated as the primary phase and oil as the secondary phase. The interfacial surface tension between the two phases was defined as 0.02 N/m, while the Carreau model was implemented to account for the fluids' non-Newtonian behavior. The boundary conditions included inlet velocities of 4.355 m/s for water and 6.349 m/s for oil, a pressure outlet, and no-slip conditions along the pipe walls. For pressure-velocity coupling, the PISO algorithm was employed, with PRESTO utilized for pressure discretization, second-order upwind for momentum, and Geo-reconstruct for volume fraction calculations. A first-order transient formulation was applied, and the simulation was initialized with an oil volume fraction of zero. The convergence criteria were established at 0.001 for both continuity and velocity residuals. The time step is 0.0001s with number of time step is 40,000.

### 2.3 Working fluids

Current work is dedicated to observing the CAF phenomenon in T-shaped pipes for heavy oil–water systems. In the annulus, water with a viscosity ($\mu w$) of 0.001 Pa

and a density ($\rho w$) of 999 kg/m$^3$ was used as lubricant fluid. The heavy oil, considered as non-Newtonian Carreau fluid, was used as the core fluid with viscosity ($\mu_0$) of 170.811 Pa. s at zero shear rate and density ($\rho_0$) of 976 kg/m$^3$.

## 2.4 Mathematics

### *2.4.1 Volume of fluid*

The Volume of Fluid (VOF) model is utilized because, according to the ANSYS user guide, it effectively prevents phase interpenetration in oil-water flow. In this model, mass and phase transfer are assumed to be negligible, and the flow is considered incompressible. As a result, the governing equations for mass and momentum conservation, as represented in Equations 2.1 and 2.2, are established to describe the flow behavior accurately.

$$\frac{\partial}{\partial t}(\rho) + \nabla \cdot (\vec{U}) = 0, \tag{2.1}$$

$$\frac{\partial}{\partial t}(\vec{U}) + \nabla \cdot (\vec{U}\vec{U}) = -\nabla P + \nabla \cdot [\mu(\nabla \vec{U} + \nabla \vec{U}^T)] + \rho \vec{g} + \vec{S}, \tag{2.2}$$

where $\vec{U}$ represents the velocity field, $\mu$ is the viscosity, $P$ is the pressure, $\vec{g}$ is the gravity vector, and $\vec{S}$ is the surface tension force. In the VOF model, the momentum equation accounts for both phases simultaneously by calculating the density and viscosity of the two-phase system using the water volume fraction ($\varepsilon_w$). This approach is represented in Eqs. (2.3)-(2.4.)

$$\rho_m = \rho_w \varepsilon_w + (1 - \varepsilon_w)\rho_0, \tag{2.3}$$

$$\mu_m = \mu_w \varepsilon_w + (1 - \varepsilon_w)\mu_0. \tag{2.4}$$

### *2.4.2 Continuum surface tension*

In this model, surface tension depends on the coefficient of surface tension ($\sigma$) and the curvature of the interface ($k$). The following equation represents surface tension in the CSF model:

$$S = \sigma k \frac{\rho \nabla a_0}{0.5(\rho_0 + \rho_w)}. \tag{2.5}$$

The curvature in the CSF model is calculated by considering the local gradient of the normal vector to the interface, defined as the gradient of the oil volume fraction $a_0$.

$$n = \nabla a_0, \ \hat{n} = \frac{n}{|n|}, \ k = \nabla \hat{n}. \tag{2.6}$$

In the CSF model, the wall adhesion effect is introduced, which is related to the contact angle between the oil and water. Therefore, the curvature equation is modified due to the contact angle as follows:

$$\hat{n} = \hat{n}_w \cos\theta_w + \hat{t}_w \sin\theta_w, \tag{2.7}$$

where $\hat{n}_w$ and $\hat{t}_w$ are the normal and tangential vectors to the pipe wall, and $\theta_w$ is the contact angle between the pipe wall and the interface.

## 2.5 Dimensionless parameter for scaling-up

Current work is using dimensionless parameters for scaling-up. Dimensionless would be an essential to bring physics phenomenon on initial size geometry to scaled-up geometry.

### *2.5.1 Bingham number*

The Bingham number represents the ratio of yield stress to viscous stress and characterizes the flow behavior of many fluids [24]. Equation 2.8 illustrates the relationship that defines the Bingham number.

$$Bm = \frac{\tau_y l_c}{\mu v}. \tag{2.8}$$

The Bingham number (Bm) is determined by several key parameters: $v$, the average fluid velocity (m/s); $\mu$, the dynamic

viscosity of the fluid (kg/ms); $\tau_y$, the yield stress (Pa); and $l_c$, the pipe length ($m$).

The Bingham number serves as a key parameter in determining flow rate, flow characteristics, and pressure loss [24]. It represents the minimum force or stress needed to initiate fluid motion. When this yield stress threshold is surpassed, the fluid transitions into a viscous state, allowing it to flow unimpeded.

#### *2.5.2 Froude number*

The Froude number represents the ratio of characteristic velocity to gravitational wave velocity.

$$Fr = \frac{v}{\sqrt{gD_{pipe}(1-\varepsilon_w)}}. \qquad (2.9)$$

The Froude number (Fr) is defined using several key parameters: $v$, the superficial mixture velocity (m/s); g, the gravitational acceleration (m/s$^2$); $\varepsilon_w$, the fraction water and $D_{pipe}$, the pipe diameter (m).

This number provides an interpretation of fluid flow behavior, which can be analyzed based on the value of the Froude number (Fr). If $Fr > 1$, the flow is faster, as inertial forces dominate over gravitational forces. Conversely, if $Fr < 1$, the flow is slower due to the greater influence of gravitational forces compared to inertia.

#### *2.5.3 Reynolds number*

The Reynolds number is a dimensionless parameter used to determine the flow regime along a pipe. For non-Newtonian fluids, the Reynolds number must be adjusted to account for the fluid's behavior, leading to the concept of the generalized Reynolds number. This adjustment primarily concerns the fluid's viscosity, which must correspond to the specific fluid model being applied. The following equation represents the generalized Reynolds number when using the Carreau model for viscosity. This equation, proposed by Bilgi & Pahlevan [25], is presented in Eq. (2.10)

$$Re = \frac{8\rho U_m^2}{\mu_\infty \frac{8U_m}{D_{pipe}} + [(\mu_0-\mu_\infty)\frac{8U_m}{D_{pipe}} \cdot [1+(\frac{8U_m}{D_{pipe}}\gamma)^2]]}. \qquad (2.10)$$

The Reynolds number (Re) is influenced by several key parameters, including density of the fluid mixture ($\rho m$) in kg/m$^3$, the mixture flow velocity ($U_m$) in m/s, and the pipe diameter ($D_{pipe}$) in meters. Additionally, viscosity plays a crucial role, with $\mu_0$ representing the viscosity at the initial shear rate and $\mu_\infty$ denoting the viscosity at the infinite shear rate. The shear rate ($\gamma$) in $s^1$ and the power-law index ($n$) further contribute to defining the flow behavior, particularly for non-Newtonian fluids.

## 3. Results and Discussion

### 3.1 Mesh quality

The number of meshes was determined through a grid independence test. For this geometry, the grid independence was previously conducted by comparing the pressure gradient values with the experimental results of Arney et al., where the experimental pressure gradient was 9.29 kPa upstream and 1.54 kPa downstream [4]. The following presents the results of the grid independence test from these two studies (Table 1).

**Table 1.** Grid independence test [4].

| Mesh | Pressure Gradient | | Reltive Error to Experiment | |
|---|---|---|---|---|
| | Upstream | Down-stream | Upstream | Down-stream |
| 54.254 | 8.87 | 3.55 | 5% | 131% |
| 182.347 | 9.56 | 1.94 | 3% | 26% |
| 328.700 | 9.39 | 1.67 | 1% | 9% |
| 509.212 | 9.5 | 1.72 | 2% | 12% |

From results on Table 1, it can be seen that the mesh with the smallest relative

error is mesh 328.700. Therefore, in this study, the number of mesh elements was set to be close to 328.700, resulting in a mesh count of 339.458. The quality of the mesh can be seen at Table 2 below.

**Table 2.** Mesh quality.

| Parameter | Min | Average | Max |
|---|---|---|---|
| Skewness | 0.00002 | 0.025 | 0.3 |
| Orthogonality | 0.56 | 0.95 | 1 |

### 3.2 Cross-sectional analysis

A key aspect of CAF behavior is the distribution of the cross-sectional area occupied by each phase, which significantly influences flow stability, pressure drop, and interfacial interactions. Analyzing the cross-sectional area provides critical insights into flow dynamics, allowing for the identification of flow regime transitions, and fouling tendencies. The interface between the core and annular phases plays a crucial role in determining the overall hydrodynamic performance, as disturbances or asymmetries can lead to instability and flow disruptions.

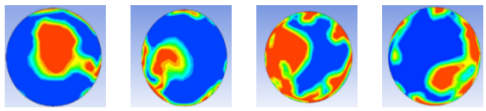


**Fig. 2.** Cross-sectional before scale-up: (a) Downstream 1 (200 mm after junction); (b) Downstream 2 (200 mm after junction); (c) Outlet 1; (d) Outlet 2.

Flow pattern on the pipe can be seen on Figs. 3, 5, 7, 9, 11, 13 and 15. These figures show that some of characteristics of each system configuration. The characteristics is CAF forms along the straight section of the pipe before passing through the junction. After passing the junction, the flow becomes unstable due to disturbances

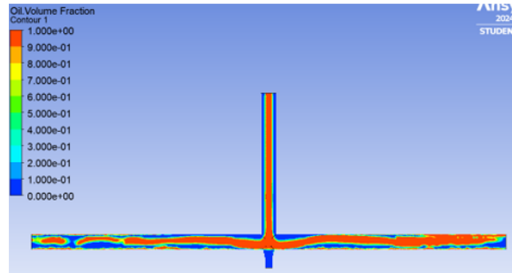


**Fig. 3.** Flow pattern geometry before scale-up.

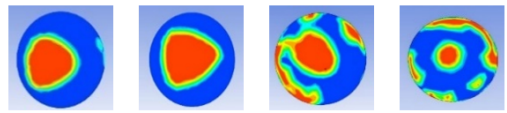


**Fig. 4.** Cross-sectional scale-up 1.5× with Fixed Reynolds Number: (a) Downstream 1 (200 mm after junction); (b) Downstream 2 (200 mm after junction); (c) Outlet 1; (d) Outlet 2.

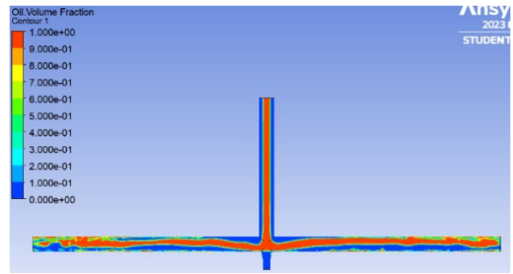


**Fig. 5.** Flow pattern geometry 1.5× with Fixed Reynolds Number.

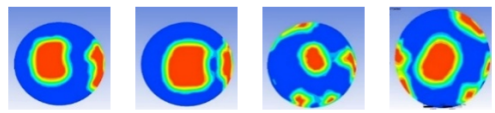


**Fig. 6.** Cross-sectional scale-up 1.5× with Fixed Bingham Number: (a) Downstream 1 (200 mm after junction); (b) Downstream 2 (200 mm after junction); (c) Outlet 1; (d) Outlet 2.

caused by changes in flow direction. In this context, water insertion plays a crucial role in restoring the flow to a concentric state.

Fouling phenomena are commonly observed during the fluid flow process, be-

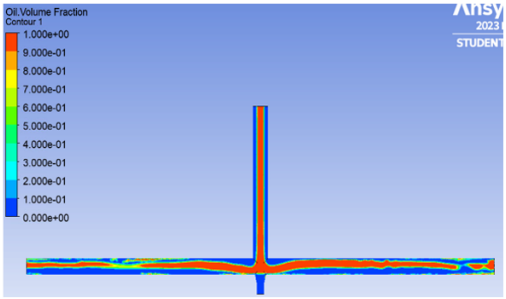


**Fig. 7.** Flow pattern geometry 1.5× with Fixed Bingham Number.

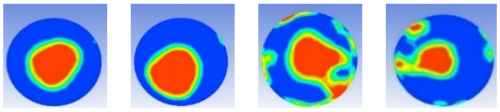


**Fig. 8.** Cross-sectional Scale-up 1.5× with Fixed Froude Number: (a) Downstream 1 (200 mm after junction); (b) Downstream 2 (200 mm after junction); (c) Outlet 1; (d) Outlet 2.

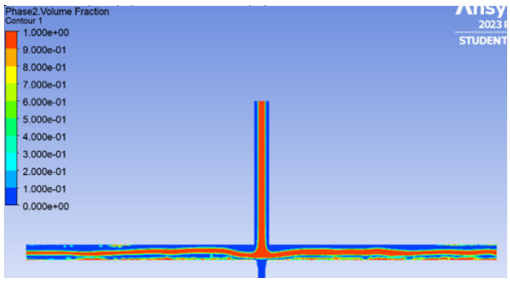


**Fig. 9.** Flow pattern geometry 1.5× with Fixed Froude Number.

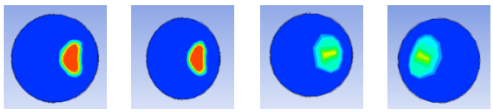


**Fig. 10.** Cross-sectional scale-up 5× with Fixed Reynolds Number: (a) Downstream 1 (200 mm after junction); (b) Downstream 2 (200 mm after junction); (c) Outlet 1; (d) Outlet 2.

ginning with a layer of oil that adheres to the internal surfaces of the pipe, as illustrated in Figs. 2, 4, 6, 8 and 10. Over

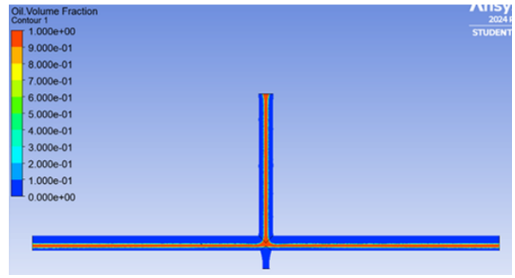


**Fig. 11.** Flow pattern geometry 1.5× with Fixed Reynolds Number.

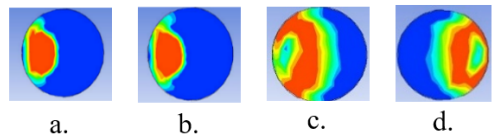


**Fig. 12.** Cross-sectional scale-up 5× with Fixed Froude Number: (a) Downstream 1 (200 mm after junction); (b) Downstream 2 (200 mm after junction); (c) Outlet 1; (d) Outlet 2.

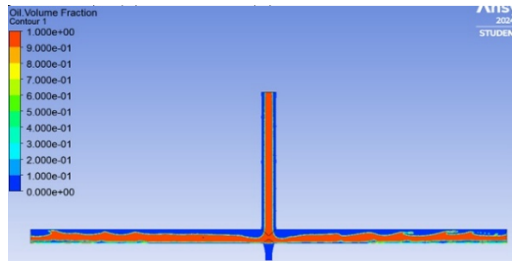


**Fig. 13.** Flow pattern geometry 5× with Fixed Froude Number.

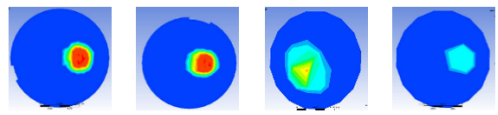


**Fig. 14.** Cross-sectional scale-up 5× with Fixed Bingham Number: (a) Downstream 1 (200 mm after junction); (b) Downstream 2 (200 mm after junction); (c) Outlet 1; (d) Outlet 2.

time, this adherence leads to the accumulation of a substantial oil layer along the pipe walls, which results in a significant increase in pressure drop. Two separate simulations carried out by Kaushik et al. [15] and

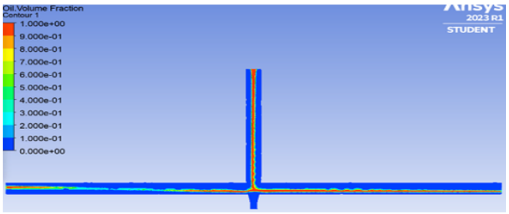


**Fig. 15.** Flow pattern geometry 5× with Fixed Bingham Number.

Babakhani Dehkordi et al. [16] investigated pipe geometries featuring abrupt changes in diameter. Their findings indicated that alterations in pipe geometry, especially when larger diameters are employed, can mitigate the tendency for fouling to occur. Simulations using pipes scaled up by a factor of 5 in diameter showed no fouling formation, except in the case of the Froude number, where the fluid velocity was higher compared to other cases.

In the base case before scale-up (Figs. 2–3), CAF is observed to form along the straight pipe section. However, after the junction, instabilities appear due to the change in flow direction. Water insertion helps re-stabilize the concentricity of the CAF core.

When scaling up by 1.5× with constant Reynolds number (Figs. 4–5), CAF formation remains visible but becomes less stable near the outlet due to the sensitivity of shear-thinning viscosity to velocity variations. At constant Bingham number (Figs. 6–7), the flow shows reduced concentricity, confirming that higher yield stress limits CAF stability by resisting interface adjustment. By contrast, maintaining a constant Froude number (Figs. 8–9) preserves concentric CAF more effectively, since inertial forces dominate over gravitational effects, counteracting stratification.

At 5× scale-up, the flow behavior diverges sharply. With constant Reynolds number (Figs. 10–11), CAF stability deteriorates, showing strong eccentricity and fouling along the wall. Under constant Froude number (Figs. 12–13), concentric CAF is largely maintained, confirming that $Fr > 1$ is critical for scale-up stability. In the Bingham number case (Figs. 14–15), severe instability and wall fouling occur, indicating that high yield stress prevents stable CAF reformation in large geometries.

Coelho et al. [1] also monitored the formation of fouling zones in experimental results using pipes with various shapes, such as branching and elbows. The pipe shape influenced fouling formation due to changes in fluid flow direction. Additionally, it is important to emphasize that, in the absence of additional levitation forces, the eccentricity of CAF increases the likelihood of oil fouling. Therefore, facilitators such as water insertion are needed to prevent fouling in pipes and to avoid the CAF flow becoming eccentric.

Additionally, the buoyancy force is unable to counterbalance the gravitational force experienced by the fluid, increasing the likelihood of fouling. The Froude number represents the resistance of an object (in this case, oil flow) in a water stream. A Froude number greater than 1 helps to maintain the concentricity of CAF flow. According to Osundare et al., when gravitational forces are more dominant, they pull the fluid flow downward, leading to stratification in the flow [9].

### 3.3 Pressure gradient result

The pressure gradient is defined as the rate of pressure change per unit length along the flow direction. In multiphase flow systems, the pressure gradient indicates the energy required to transport fluids through the pipeline, and it is strongly influenced by viscosity, flow regime, pipe geometry, and

interfacial interactions between phases.

The pressure gradient is a key factor for the efficiency and stability of the flow system. CAF involves a high-viscosity oil core surrounded by a lower-viscosity annular fluid, which reduces frictional resistance along the pipe walls. This flow pattern leads to a lower pressure gradient compared to single-phase heavy oil transport, which minimizes energy losses and optimizes pipeline performance [22].

The following is a comparison of the pressure gradient from the simulation results with the calculated results based on Equation from Arney et al. [17] in the Junction area, as shown in Table 3.

The pressure gradient influences the formation of interface waves. A higher-pressure gradient will result in larger and more energetic interface waves between the core and annular phases. The velocity of both the core and annular phases is enhanced as a result. As reported by Xie et al. [18], an increase in the superficial velocities of oil and water corresponds to a rise in the frictional pressure gradient. Furthermore, the pipe diameter plays a crucial role in this gradient, as it directly influences velocity distribution. The geometric characteristics of the pipeline also contribute to variations in the pressure gradient. Notably, branching has an adverse downstream effect, leading to an elevation in the frictional pressure gradient [19].

Comparison between the pressure gradient values from CFD simulations and theoretical equations is conducted to validate whether the simulation model is accurate. In some cases, such as Bingham fluids, the error is quite high due to the improper parameters used, which fail to account for consistent treatment of the wall shear value. This results in changes in viscosity. Wall shear can affect the viscosity of shear-thinning fluids by altering the microscopic structure of the fluid at the interface layer, potentially impacting the flow profile and causing phenomena like slip [23]. Bingham scaling produced large errors (52–76%). This is due to the sensitivity of yield stress to shear rate near the wall. The CFD captures localized variations in viscosity and slip phenomena, while the simplified analytical model cannot.

For the Reynold's case, the error is relatively large compared to other cases, primarily because the fluid used exhibits shear-thinning behavior. In the Reynold's case, the oil viscosity is assumed to be constant at inlet the pipe, but this assumption is incorrect, as oil viscosity changes with the shear rate in the pipe. Thus, it cannot be considered the same for all positions. Reynolds-based scaling produced very large discrepancies (up to 554% at 5×). This arises because shear-thinning fluids do not maintain constant viscosity; the analytical model assumes constant viscosity, leading to unrealistic underprediction of wall shear effects.

In the Froude's case, the pressure gradient and Froude number influence the fluid phase distribution within the pipe, as the pressure gradient affects the formation of interface waves. The error in the Froude's case ranges from 26% to 35%. Its happen because of Froude scaling provides a foundational approach for modeling two-phase flows like core-annular flow, its limitations necessitate the consideration of additional factors such as interfacial tension and viscous effects. Therefore, need another alternative approach to more accurate predictions and better design of CAF systems.

Thus, the large percentage errors are not only numerical but also reflect fundamental limitations of analytical models that

neglect shear-thinning rheology, and transient instabilities.

#### *3.3.1 Oil holdup result*

Oil holdup is defined as the volumetric fraction of oil relative to the total cross-sectional area of the pipe in a multiphase flow system. It quantifies the proportion of oil occupying the flow channel at a given location and time, and it is a key parameter for evaluating flow stability, energy efficiency, and phase distribution in core annular flow (CAF).

The oil holdup ratio is a crucial parameter in multiphase flow systems, especially in Core Annular Flow (CAF), where a high-viscosity oil is transported within a lower-viscosity water annulus. This ratio represents the volumetric fraction of oil in the total cross-sectional area of the pipe, significantly affecting flow stability, pressure drop, and energy efficiency [3, 21].

The following is a comparison of the holdup ratio from simulation results with the holdup ratio calculated using the Arney equation from Arney et al. [17] presented in Table 4. According to the literature, holdup values depend on the oil's superficial velocity, with oil velocity being higher in smaller pipes (Re and Bn) due to variations. Consequently, a lower holdup value will occur with higher superficial oil velocities. However, if the oil velocity falls below a certain threshold, CAF will not form. Based on Table 4, errors remain moderate (0–20%) in 1.5x scale-up but increase dramatically (up to 67%) at 5x scale-up under Reynolds and Bingham scaling. Physically, this is due to at large scales, oil viscosity decreases more strongly with velocity, causing thinner oil layers in CFD than predicted by models. The Arney equation does not account for viscosity dependence, making it less reliable for non-Newtonian systems. At higher diameters, stratification increases and the CAF core becomes eccentric, leading to lower holdup than predicted. The holdup ratio for the 5x scale-up pipe, with a higher Froude number than the original size and the 1.5x scale-up, increases due to changes in the cross-sectional area and the feed velocity of water and oil. These velocities influence the holdup accumulation, as adjusting both values results in a relative error approaching 0%, consistent with Arney et al. [17], who stated that the holdup ratio correlates with the superficial velocities of water and oil. Similarly, in the 1.5x scale-up case, the holdup ratio increases due to the need to increase velocity to maintain the Froude number, which theoretically leads to an increase in the holdup ratio. Joseph et al. [20] also indicated that the holdup ratio correlates with the superficial velocities of water and oil.

Furthermore, for other dimensionless parameters in the simulation, a decrease in the holdup ratio can be observed. This is due to the need to reduce the oil feed velocity to adjust the dimensionless numbers, which in turn lowers the oil's superficial velocity, leading to a reduction in the holdup ratio.

The relatively high error observed in some cases is due to factors such as shear-thinning behavior. In smaller pipes, this effect is less noticeable, but in the 5x scale-up pipe, shear-thinning causes the oil flow to thin out, reducing the simulation results. Meanwhile, the Arney equation does not account for viscosity, which significantly affects the holdup ratio.

### 3.4 Energy evaluation

Assessing energy performance in core annular flow (CAF) is essential for evaluating its effectiveness as a fluid transport technique, particularly for high-

**Table 3.** Pressure gradient comparison.

| Simulation | Pressure Gradient Downstream (kPa/m) | | Error |
|---|---|---|---|
| | CFD | Calculation | |
| Pipe T Water Insertion Before Scale-up | 57.2449 | 73.9533 | 23% |
| Scale-up 1.5× Geometry with Fixed Reynolds Number | 19.6607 | 24.3767 | 19% |
| Scale-up 1.5× Geometry with Fixed Bingham Number | 11.5938 | 24.1089 | 52% |
| Scale-up 1.5× Geometry with Fixed Froude Number | 23.5341 | 31.8456 | 26% |
| Scale-up 5× Geometry with Fixed Reynolds Number | 30.4494 | 4.6540 | 554% |
| Scale-up 5× Geometry with Fixed Froude Number | 17.3528 | 12.8578 | 35% |
| Scale-up 5× Geometry with Fixed Bingham Number | 0.4203 | 1.7612 | 76% |

viscosity oil applications. This flow regime enhances energy efficiency by forming a lubricating annular layer composed of a lower-viscosity fluid, which significantly reduces friction between the oil core and the pipe wall.

In Table 5, $\nabla P^*$ is pressure drop reduction (%), Es is energy consumption one phase fluid (Joule/m$^3$), and Eb is energy consumption multiphase fluid (Joule/m$^3$)..

Consequently, the resulting decrease in shear stress leads to a notable reduction in pressure drop, thereby minimizing the pumping power required in comparison to conventional single-phase oil transport. The overall energy savings achieved through CAF are influenced by multiple factors, including the viscosity contrast between the core and annular phases, pipeline geometry, and prevailing flow conditions [1]. To quantify these benefits, key parameters such as pressure gradient, power reduction factor, and pump energy consumption are analyzed. Computational Fluid Dynamics (CFD) simulations provide insights into how scaling up CAF systems impacts energy efficiency, helping to optimize pipeline design for industrial applications. The following are the calculation results comparing the energy savings achieved by CAF with single-phase oil flow in the pipeline, as shown in Table 5.

## 4. Conclusion

The formation of CAF is influenced by several key dimensionless parameters. First, the Bingham number, which plays a critical role, is highly dependent on the velocity and shear of the fluid. The Froude number, similarly, is influenced by fluid velocity, and its reliability is highlighted by simulation results that show a relatively lower error compared to other parameters. The Reynolds number, on the other hand, is significantly affected by the fluid's viscosity and velocity.

Reynolds number (Re) primarily governs inertial–viscous interactions. While useful in smaller pipes, scaling by Re fails in large diameters because viscosity in shear-thinning fluids is not constant. This leads to overestimation of stability in analytical models. Bingham number (Bn) controls yield stress effects. High Bn increases resistance to interface reformation, reducing CAF stability. Scaling with Bn at larger diameters results in excessive fouling and unstable cores. Froude number (Fr) balances inertial and gravitational forces. Maintaining $Fr > 1$ ensures concentric CAF flow even in large pipes, making it the most reliable criterion for scale-up.

The stability of CAF in larger pipes, as demonstrated by the simulation, depends on a combination of factors, most notably the superficial velocity and viscosity of the

**Table 4.** Oil holdup comparison.

| Simulation | Oil Holdup Downstream | | Error |
|---|---|---|---|
| | CFD | Calculation | |
| Pipe T Water Insertion Before Scale-up | 0.3768 | 0.3355 | 12% |
| Scale-up 1.5× Geometry with Fixed Reynolds Number | 0.3181 | 0.3190 | 0% |
| Scale-up 1.5× Geometry with Fixed Bingham Number | 0.1764 | 0.2145 | 18% |
| Scale-up 1.5× Geometry with Fixed Froude Number | 0.3104 | 0.3820 | 19% |
| Scale-up 5× Geometry with Fixed Reynolds Number | 0.1314 | 0.3510 | 63% |
| Scale-up 5× Geometry with Fixed Froude Number | 0.4169 | 0.4170 | 0% |
| Scale-up 5× Geometry with Fixed Bingham Number | 0.1164 | 0.3510 | 67% |

**Table 5.** Energy evaluation.

| Simulation | Eb | Es | $\nabla P^*$ | Energy Saving |
|---|---|---|---|---|
| Pipe T Water Insertion Before Scale-up | 79 | 958 | 92% | 92% |
| Scale-up 1.5× Geometry with Fixed Reynolds Number | 38 | 418 | 91% | 91% |
| Scale-up 1.5× Geometry with Fixed Bingham Number | 7 | 420 | 98% | 98% |
| Scale-up 1.5× Geometry with Fixed Froude Number | 27 | 310 | 91% | 91% |
| Scale-up 5× Geometry with Fixed Reynolds Number | 614 | 3,428 | 40% | 82% |
| Scale-up 5× Geometry with Fixed Froude Number | 88 | 1,213 | 91% | 93% |
| Scale-up 5× Geometry with Fixed Bingham Number | 7 | 1,487 | 98% | 100% |

fluid.

In terms of energy efficiency, CAF technology proves to be highly effective, offering energy savings more than 80% when compared to single-phase oil flow.

## References


[1] Dianita C, Piemjaiswang R, Chalermsinsuwan B. Computational fluid dynamics approach for energy savings evaluation in core annular flow of a horizontal T-pipe. Energy Rep. 2023 Jun 3;9:8–15.

[2] Dianita C, Piemjaiswang R, Chalermsinsuwan B. CFD simulation and statistical experimental design analysis of core annular flow in T-junction and Y-junction for oil-water system. Chem Eng Res Des. 2021 Dec;176:279–95.

[3] Dianita C, Piemjaiswang R, Chalermsinsuwan B. Effect of T- and Y-Pipes on core annular flow of Newtonian/Non-Newtonian Carreau fluid using computational fluid dynamics and statistical experimental design analysis. Iran J Sci Technol Trans Mech Eng. 2022 Dec 14;47(3):941–58.

[4] Dianita C, Piemjaiswang R, Chalermsinsuwan B. Recovery of core annular flow structure in a horizontal T-pipe using CFD approach. Alex Eng J. 2023 Aug;77:553–66.

[5] Skadsem HJ, Leulseged A, Cayeux E. Measurement of drilling fluid rheology and modeling of thixotropic behavior. Appl Rheol. 2019 Mar 1;29(1):1–11.

[6] Pratama MF. Simulasi dinamika fluida komputasi penggandaan skala pipa horizontal dengan pelebaran penampang pada aliran core annular menggunakan parameter tak berdimensi [Undergraduate thesis]. Depok: University of Indonesia; 2023.

[7] Dianita C. Application of core annular flow for oil transportation in different pipe configurations using computational fluid dynamics [Doctoral dissertation]. Bangkok: Chulalongkorn University; 2022.

[8] Montes D, Cortés FB, Franco CA. Reduction of heavy oil viscosity through ultrasound cavitation assisted by NiO nanocrystals-functionalized $SiO_2$ nanoparticles. DYNA. 2018 Oct 1;85(207):153–60.

[9] Sherman SG, Becnel AC, Wereley NM. Relating Mason number to Bingham number in magnetorheological fluids. J Magn Magn Mater. 2015 Apr;380:98–104.

[10] Bilgi C, Pahlevan NM. Viscosity-model-independent generalized Reynolds number for laminar pipe flow of shear-thinning and viscoplastic fluids. Eur J Mech B Fluids. 2024 Jun 1;107:.

[11] Kaushik VVR, Ghosh S, Das G, Das PK. CFD simulation of core annular flow through sudden contraction and expansion. J Pet Sci Eng. 2012 May;86–87:153–64.

[12] Babakhani Dehkordi P, Azdarpour A, Mohammadian E. The hydrodynamic behavior of high viscous oil–water flow through horizontal pipe undergoing sudden expansion—CFD study and experimental validation. Chem Eng Res Des. 2018 Nov;139:144–61.

[13] Coelho NMDA, Elena M, Mota N, Lia L,Santos AR, Renato L, et al. Energy savings on heavy oil transportation through-core annular flow pattern: An experimental approach. Int J Multiph Flow. 2019Oct 11;122:103127.

[14] Osundare OS, Falcone G, Lao L, Elliott A. Liquid–liquid flow pattern prediction using relevant dimensionless parameter groups. Energies. 2020 Aug 24;13(17):4355.

[15] Hu H, Jing J, Tan J, Yeoh GH. Flow patterns and pressure gradient correlation for oil–water core–annular flow in horizontal pipes. Exp Comput Multiph Flow. 2019 Oct 11;.

[16] Arney MS, Bai R, Guevara E, Joseph DD, Liu K. Friction factor and holdup studies for lubricated pipelining—I. Experiments and correlations. Int J Multiph Flow. 1993 Dec;19(6):1061–76.

[17] Xie B, Jiang F, Lin H, Zhang M, Gui Z, Xiang J. Review of core annular flow. Energies. 2023 Feb 2;16(3):1496.

[18] Jing J, Yin X, Mastobaev BN, Valeev AR, Sun J, Wang S, et al. Experimental study on highly viscous oil–water annular flow in a horizontal pipe with 90° elbow. Int J Multiph Flow. 2021 Feb;135:103499.

[19] Schryver RD, El Cheikh K, Lesage K, Yardimci MY, Schutter GD. Numerical reliability study based on rheological input for Bingham paste pumping using a finite volume approach in OpenFOAM. Materials. 2021 Sep 2;14(17):5011.

[20] Andrade T, Silva F, Neto S, Lima A. Applying CFD in the analysis of heavy oil-water two-phase flow in joints by using-core annular flow technique. Int J Multiphys. 2013 Jun;7(2):137–52.

[21] Yin X, Li J, Shen J, Huang X, Zhou F, Zhao Z, et al. Study on the flow characteristics of heavy oil–water two-phase flow in the horizontal pipeline. ACS Omega. 2024 May 29;9(23):24396–405.

[22] Joseph DD, Bai R, Chen KP, Renardy YY. Core–annular flows. Annu Rev Fluid Mech. 1997 Jan;29(1):65–90.